nature nanotechnology

LETTERS

PUBLISHED ONLINE: 5 JULY 2009 | DOI: 10.1038/NNANO.2009.177

Measurement of the quantum capacitance of graphene

Jilin Xia[1], Fang Chen[1], Jinghong Li[2]* and Nongjian Tao[1]*

Graphene has received widespread attention due to its unique electronic properties[1–5]. Much of the research conducted so far has focused on electron mobility, which is determined by scattering from charged impurities and other inhomogeneities[6,7]. However, another important quantity, the quantum capacitance, has been largely overlooked. Here, we report a direct measurement of the quantum capacitance of graphene as a function of gate potential using a three-electrode electrochemical configuration. The quantum capacitance has a non-zero minimum at the Dirac point and a linear increase on both sides of the minimum with relatively small slopes. Our findings—which are not predicted by theory for ideal graphene—suggest that charged impurities also influences the quantum capacitance. We also measured the capacitance in aqueous solutions at different ionic concentrations, and our results strongly indicate that the long-standing puzzle about the interfacial capacitance in carbon-based electrodes has a quantum origin.

The electron transport properties of graphene devices are critical to many applications, but our understanding of these properties is still incomplete, in spite of rapid advances in recent years. One unsolved puzzle is the minimum in the conductivity at the Dirac point, which has stimulated many recent theoretical and experimental efforts[8,9]. It has been proposed that this minimum is due to charged impurities that induce puddles[6] of electrons and holes in the graphene. To fully understand the transport properties, it is important to investigate the scattering of the carriers by the impurities, and also the density of carriers at and near the Dirac point (which is related to the quantum capacitance). Electron transport in graphene has been studied using the field-effect transistor (FET) configuration, in which a graphene sample is placed on an oxidized silicon substrate and connected to source and drain electrodes, and the current through the graphene controlled with a back gate. The capacitance in these devices is dominated by the capacitance of the oxide layer, which makes it difficult to determine the quantum capacitance. However, to decrease the operation voltage, it is expected that the oxide layers in future devices will be much thinner and have higher values of dielectric constant k, which means that the quantum capacitance will eventually be the dominant source of capacitance. Others[10] have reported an effort to determine the quantum capacitance of graphene. Owing to the large contribution from the gate oxide and trap capacitance contributions in the top-gate device, their measured capacitance is an order of magnitude smaller than the quantum capacitance. In the present work the use of an electrochemical gate and ionic liquid reduces the Debye ionic screening length to a few ångströms, which makes the quantum capacitance a dominant component of the measured capacitance. We also provide a simple theory with only one parameter (impurity concentration) to quantitatively explain the measured quantum capacitance.

As well as electronic applications, graphite and other carbon-based electrodes have already found broad applications in analytical chemistry, electrochemistry, batteries, chemical sensors and biosensors. The interfacial capacitance, a basic quantity in these applications, is unusually small (compared with metal electrodes) and has a peculiar V-shape. Measuring the quantum capacitance of single- and few-layer graphene in electrolytes will shed new light on these puzzling aspects of the interfacial capacitance of carbon electrodes.

An expression for the quantum capacitance of a perfect graphene sheet has been derived[11,12], but direct measurements that can be compared with theory are still lacking. Other groups[13] have studied the local capacitive properties of graphene using scanning probe microscopy (SPM). Absolute capacitance values per unit area were difficult to obtain because the SPM tip geometry was unknown and variable, and the quantum capacitance contribution was negligibly small compared to the capacitance contribution from the thick oxide used in the experiment. In the present work, we measure the quantum capacitance of single-layer graphene in an ionic liquid electrolyte. The ionic liquid is chemically inert and stable and, more importantly, its Debye ionic screening length is virtually zero, which makes the quantum capacitance a dominant source of the measured capacitance. We are thus able to determine the absolute values of graphene capacitance as a function of voltage, and compare the experimental results with theoretical predictions. To resolve the peculiar interfacial capacitance of carbon electrodes, we also study the capacitance of graphene in aqueous solutions at different ionic concentrations.

Figure 1 shows the experimental setup, in which a graphene sheet supported on a silicon/SiO_2 (290 nm) substrate is connected to a chromium (5 nm)/gold (80 nm) electrode. The graphene surface is covered by a thick photoresist layer (~4.5 μm) except for a small window with a diameter of 10 μm, which exposes the electrolyte. This configuration minimizes the background capacitance and prevents exposure of the graphene edges to the electrolyte. The interfacial capacitance of the graphene was measured using the standard three-electrode electrochemical cell using a potentiostat in which the potential of graphene is controlled with respect to a reference electrode (a platinum electrode). The inset of Fig. 1 shows an optical image of the device with one electrode; the distinct colour of the sample, together with Raman spectroscopy, provides accurate identification of single-layer graphene (or bilayer graphene; see Supplementary Information). Before measuring the capacitance, each device was cleaned and annealed at 200 °C in an argon/hydrogen environment[14,15] to remove contaminations arising from device fabrication. An alternative device configuration, in which the graphene is connected to two electrodes, is also used. The alternative configuration provides the additional flexibility to pass a current along the graphene

[1]Center for Bioelectronics and Biosensors, Biodesign Institute, Department of Electrical Engineering, Arizona State University, Tempe, Arizona 85287, USA, [2]Department of Chemistry, Tsinghua University, Beijing 100084, China. *e-mail: njtao@asu.edu; jhli@mail.tsinghua.edu.cn

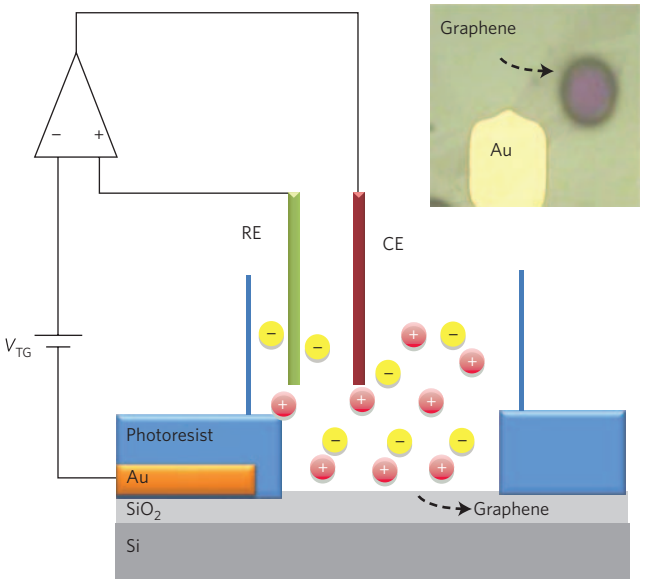

Figure 1 | Single-layer graphene device. Schematic of the quantum capacitance measurement setup in which a graphene sheet on a silicon/SiO_2 substrate is connected to a gold electrode. The edge of the graphene sheet is covered with an insulation layer so that only the top surface is exposed to an ionic liquid electrolyte. The potential of the graphene is controlled and varied with respect to a platinum reference electrode (RE) using a three-electrode electrochemical configuration. V_{TG}, electrochemical gate voltage. The inset is an optical micrograph of the graphene device. CE; counter electrode (see Methods).

sheet to remove contaminations. Both one- and two-electrode approaches produce similar results.

Figure 2a shows the capacitance versus gate potential measured in 1-butyl-3-methylimidazolium hexafluorophosphate (BMIM-PF_6), an ionic liquid. A Raman spectrum used to verify the thickness is shown in Fig. 2b. Owing to the high ionic concentration of the ionic liquid (2.9×10^{21} cm^{-3}), the Debye length approaches zero, so the measured capacitance consists of only two contributions: interfacial capacitance arising from the double layer formed by ions at the graphene–ionic liquid interface and the quantum capacitance of graphene. The two can be modelled as two capacitors in series, with the smaller of the two capacitances dominating the total capacitance. The double layer arises from the accumulation of a layer of counter-ions on a charged electrode, which is modelled by a parallel plate capacitor for which the capacitance per unit area is given by $\varepsilon_0\varepsilon/t$, where $\varepsilon_0 = 8.85 \times 10^{-12}$ F m^{-1}, ε is the dielectric constant of the ionic liquid, and t is the radius of the counter-ions. For BMIM-PF_6 ionic liquid, $\varepsilon \approx 7$ (ref. 16) and $t \approx 0.3$ nm, which leads to a double-layer capacitance of $\sim$21 μF cm^{-2}.

We measured the double-layer capacitance directly using the same experimental setup (see Supplementary Information). The measured double-layer capacitance is $\sim$21 μF cm^{-2} and changes within $\pm$3% within the gate voltage window; this is consistent with the model. These results are also in good agreement with a previous report[16]. The double-layer capacitance is large compared to the theoretically predicted quantum capacitance of graphene. Furthermore, the double-layer capacitance is not strongly dependent on the potential, making it straightforward to determine the quantum capacitance (red line in Fig. 2a).

We also used the same procedure to measure the quantum capacitance of bilayer graphene (see Supplementary Information). To establish a theoretical prediction of quantum capacitance for ideal graphene, the expression for quantum capacitance was

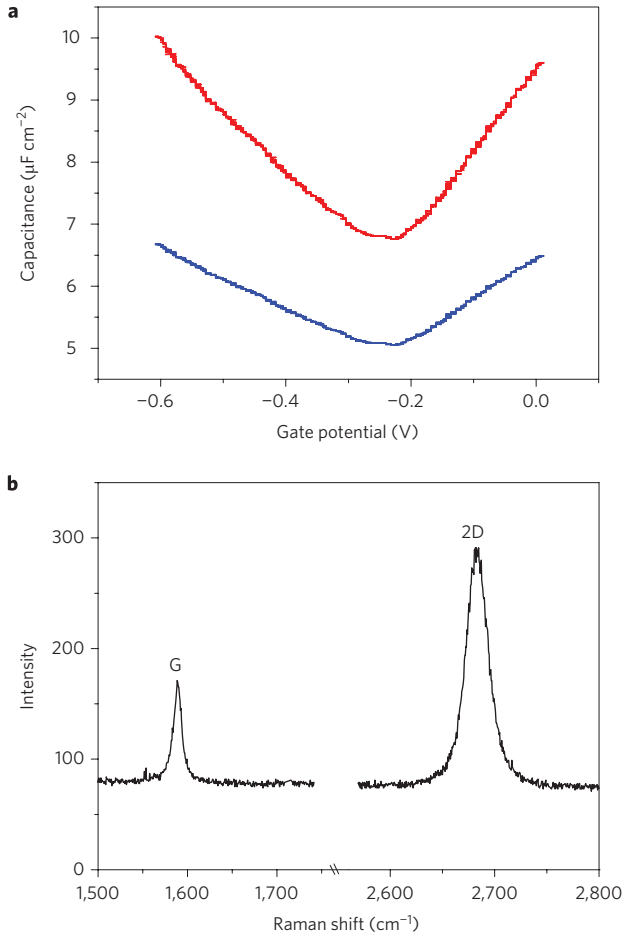

Figure 2 | Capacitance of graphene as a function of gate potential. a, Total capacitance (blue line) and quantum capacitance (red line) of graphene measured in ionic liquid BMIM-PF_6. The potential is measured with respect to a platinum quasi-reference electrode. **b**, Raman spectrum of the single-layer graphene device showing G and 2D bands.

derived based on a two-dimensional, free-electron gas model taking the form of[12]

$$C_Q = \frac{2e^2 k_B T}{\pi(\hbar v_F)^2} \ln\left[2\left(1 + \cosh\frac{eV_{ch}}{k_B T}\right)\right] \quad (1)$$

where $\hbar$ is the Planck constant, e the electron charge, k_B the Boltzmann constant, $v_F \approx c/300$ the Fermi velocity of the Dirac electron, and $V_{ch} = E_F/e$ is the potential of graphene. When $eV_{ch} \gg kT$, equation (1) reduces to[7]

$$C_Q \approx e^2 \frac{2}{\pi}\frac{eV_{ch}}{(\hbar v_F)^2} = \frac{2e^2}{\hbar v_F \sqrt{\pi}}\sqrt{n} \quad (2)$$

where n is the carrier concentration. The theory provides a quantitative description of graphene quantum capacitance in terms of Fermi velocity, carrier density temperature and fundamental physical quantities (blue circles in Fig. 3a). Several important features are worth noting. First, the quantum capacitance has a minimum value at the Dirac point. Second, the minimum value is close to zero. Third, the capacitance increases linearly with V_{ch} with a slope of 23 μF cm^{-2} V^{-1}. Finally, it is symmetric with respect to the Dirac point.

To compare the measured capacitance with theory, the experimental result in Fig. 3b (blue symbols) is plotted again in terms

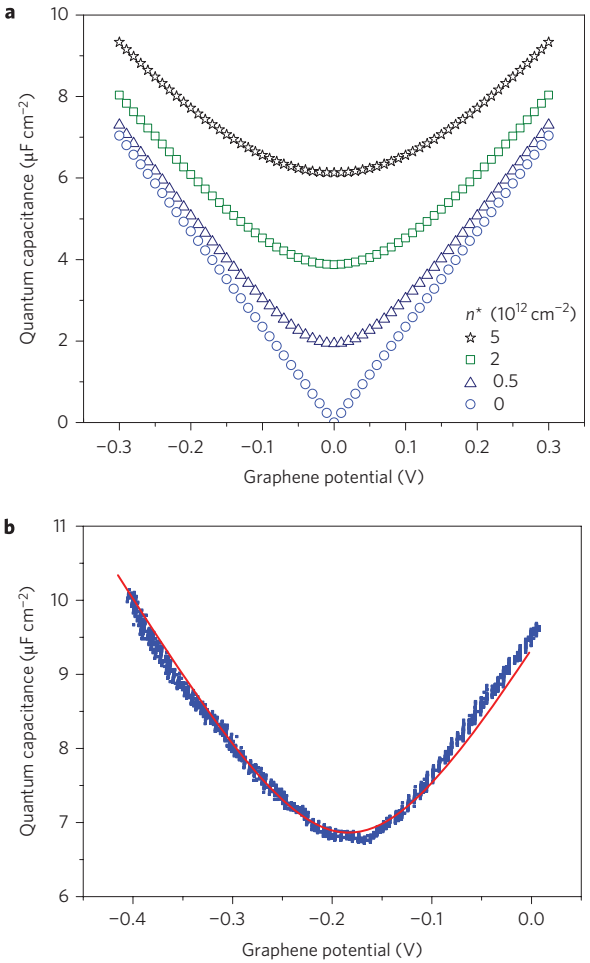

Figure 3 | Dependence of quantum capacitance on graphene. a, Simulated capacitance at different effective charged impurities n^* (0, 0.5, 2 and 5 × 10^{12} cm^{-2} from bottom to top). **b**, Fitting the measured capacitance (blue symbols) with theory (red line).

of V_{ch}, given by $V_{ch} = V_g C_i/(C_i + C_g)$, where V_g is the gate potential and $C_i = 20$ μF cm^{-2} is the double layer capacitance of the ionic liquid[16]. The measured quantum capacitance also has the V-shaped plot, and the absolute values are close to the theoretical prediction. However, there are several distinct discrepancies. First, the measured quantum capacitance minimum is round, which is more significant than would be expected from thermal smearing at room temperature. Second, the measured minimum is much greater than the predicted value of $C_{Q,min} = 2e^2 k_B T/\pi(\hbar v_F)^2 \ln(4) \sim 0.8\mu F/cm^2$ (thermal induced). Third, the measured slope is about 11 μF cm^{-2} V^{-1}, which is only about half of the predicted value.

The theoretical model is based on the assumption of pure and perfect graphene. In reality, various impurities and defects exist, and recent theoretical and experimental results have shown that charged impurities have a key role in the transport properties of graphene near the Dirac point[17,18]. It has been reported that charged impurities in substrates cause local potential fluctuations and electron/hole puddles in graphene[18,19]. The potential fluctuations based on a self-consistent theory give rise to an additional carrier density n^* induced by the impurities. In the absence of a microscopic capacitance theory that includes local potential fluctuations we can, as an approximation, take the additional carrier density into account by expressing the total carrier concentration as

$$n = |n_G| + |n^*| \quad (3)$$

where n_G and n^* are the carrier concentrations caused by the gate potential and charged impurities, respectively. Consequently, the quantum capacitance is given by

$$C_Q = \frac{2e^2}{\hbar v_F \sqrt{\pi}} (|n_G| + |n^*|)^{1/2} \quad (4)$$

Note that[7]

$$n_G = \left(\frac{eV_{ch}}{\hbar v_F \sqrt{\pi}}\right)^2 \quad (5)$$

Combining equations (4) and (5), we can calculate the quantum capacitance of graphene as a function of potential of graphene at different impurity densities.

The inclusion of the impurity contribution explains the experimental results well. First, at zero potential, $n_G = 0$ and the quantum capacitance is finite and determined by the effective or residual carrier concentration n^* (ref. 18). Second, the slopes of the linear regimes on both sides of the capacitance minimum are reduced by the charged impurities. Finally, the capacitance minimum regime is round. To further illustrate the importance of the charged impurities, numerical simulation of the quantum capacitance at different impurity densities was performed (Fig. 3a). The results show that as n^* increases, the minimum capacitance value increases, the minimum region becomes increasingly round, and the slopes decrease. We also fit the experimental results using equation (4) (red line in Fig. 3b), which gives $n^* \approx 8 \times 10^{11}$ cm^{-2}. Note that a constant of ~4 μF cm^{-2} representing the background capacitance from the electrodes and leads is included in the fitting. This value is of the same order of magnitude as the background capacitance estimated using a device containing no graphene. Note also that the position of the measured capacitance minimum occurs at −0.17 V (measured against the platinum reference electrode). This value is arbitrary, depending on the reference electrode, and only the potential change relative to the reference electrode is significant.

Based on self-consistent theory[18], n^* should be effective charged impurity concentration (or induced residual charged impurity concentration), which is related to n_{imp}, the impurity density, and is given, according to self-consistent theory[18,20,21], by

$$n_{imp} = \frac{n*}{[2r_s^2 C_0^{RPA}(r_s, a = 4d\sqrt{\pi n^*})]} \quad (6)$$

where $r_s = 2e^2/\hbar v_F(\varepsilon_1 + \varepsilon_2)$, C_0^{RPA} is the correlation function from the random phase approximation (RPA), and d (~1 nm) is the average distance from the charged impurity to graphene. $\varepsilon_1 = 3.9$ and $\varepsilon_2 = 7$ are the dielectric constants of SiO_2 and ionic liquid BMIM-PF_6 (ref. 16), respectively, which gives a value of r_s of 0.364. Using these parameters and the fitting result $n^* \approx 8 \times 10^{11}$ cm^{-2}, we determine $n_{imp} = 8.6 \times 10^{12}$ cm^{-2}. This level of charged impurities is reasonable for graphene supported on SiO_2 (refs 18 and 22).

To determine whether the peculiar interfacial capacitance of the carbon electrodes has a quantum origin, we measured the capacitance of graphene in aqueous NaF solution. We chose NaF as the electrolyte because it is commonly used for interfacial capacitance measurements; both Na^+ and F^- ions are chemically inert and do not specifically adsorb on the graphene surface. Figure 4 shows the capacitance–potential curves at different ionic concentrations of the same device. Both the shape and magnitude of the capacitance measured in the aqueous electrolyte are similar to those in the ionic liquid. An important difference is the dependence of the capacitance on the ionic concentration. In aqueous solution, the

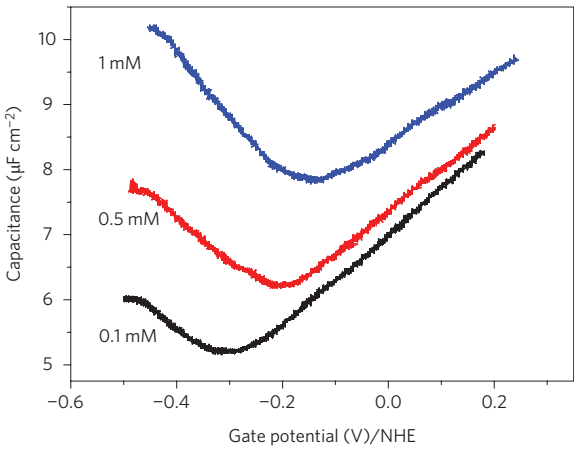

Figure 4 | Capacitance of graphene in aqueous solution. Capacitance of graphene measured in NaF aqueous solution at different ionic concentrations (0.1, 0.5 and 1 mM, from bottom to top). The potential is quoted with respect to the widely used NHE (normal hydrogen electrode) reference electrode.

double-layer capacitance is 10–20 μF cm^{-2} (ref. 23), independent of ionic concentration. However, different from the ionic liquid, the Debye lengths of the aqueous electrolytes are much greater, which leads to an additional diffuse-layer capacitance[24] contribution to the total capacitance. This diffuse-layer capacitance is known to depend on the ionic concentration, which is likely the reason for the upward shift of capacitance with concentration[23,25]. Increasing the ionic concentration also causes a positive shift in the position of the capacitance minimum. We have recently carried out a systematic study of the transport properties of graphene versus gate voltage at various ionic concentrations, and found that the effective density of charged impurities decreases with ionic concentration due to screening[26]. The positive shift in capacitance observed here can also be explained in terms of the ionic screening.

In contrast to metal electrodes, the interfacial capacitance of carbon-based electrodes, including the single-crystal basal plane of graphite, is not only an order of magnitude smaller but also shows greater variability depending on the impurity level of the materials. The unusual capacitance is explained in terms of space charge capacitance[23,25]. However, the space charge capacitance theory developed for semiconductors cannot explain the shape of the capacitance curves. Another serious difficulty for the space charge capacitance model is that the Debye length of the graphite is comparable to the lattice dimension owing to the high carrier concentrations found in graphite[23].

One of the most carefully measured systems is the basal plane of graphite by Randin and Yeager[23,25]. Its interfacial capacitance is remarkably similar to the quantum capacitance of a single-layer graphene, as well as that of bilayer graphene (see Supplementary Information). All of them have a capacitance minimum and linear increase on both sides of the minimum, the capacitance values and slopes of the linear regimes are close, and the capacitance curve shifts upwards with ionic concentration in both graphene and graphite. This level of similarity suggests that the quantum capacitance model provides a natural and quantitative explanation of the mysterious interfacial capacitance of graphite and other carbon electrodes. The modified quantum capacitance model also explains the sensitive dependence of the carbon electrodes on impurities. Finally, the quantum capacitance model is consistent with the recent observation of Dirac fermions or two-dimensional electron and hole gases at the surface of graphite[27]. However, a complete interfacial capacitance theory including both the quantum contribution and impurities is yet to be developed.

In summary, we have measured the quantum capacitance of graphene (single- and bilayer samples) as a function of gate potential. The plot of quantum capacitance versus gate potential has a symmetric V-shape with a minimum at the Dirac point, which agrees with the theoretical model developed for ideal graphene. The absolute values of quantum capacitance are also close to the theoretical prediction. However, there are several significant discrepancies between the disorder-free theory and our experiment. First, the minimum quantum capacitance at the Dirac point is finite and non-universal, which is in sharp contrast to the small value (0.8 μF cm^{-2}) predicted by the theory. Second, the minimum capacitance regime is round. Finally, the quantum capacitance increases linearly with potential on both sides of the minimum, but the slopes are smaller than the theoretical prediction. The discrepancies can be explained naturally by including charged impurities in the model. The findings underscore the importance of charged impurities for both mobility and quantum capacitance, and also support the local impurity-induced electron and hole puddle picture in graphene. Measurements of quantum capacitance also allow impurity concentrations to be determined, and measurements in aqueous solutions at different ionic concentrations indicate that the quantum capacitance is the origin of the puzzling interfacial capacitance behaviour observed in carbon-based electrodes.

Methods

Graphene was obtained by mechanical exfoliation of Kish graphite using electronic-grade dicing tape to reduce contaminations[28]. A silicon chip coated with a 290-nm-thick SiO_2 layer was used as the substrate, because single-layer graphene is known to develop a distinct colour contrast that can be easily identified under an optical microscope[29,30]. An electrochemical gate potential was applied to the graphene with respect to a platinum quasi-reference electrode inserted in the electrolyte and controlled by a potentiostat (Model 283, Princeton Applied Research). The potential in the case of aqueous electrolytes was calibrated against the widely used Ag/AgCl electrode. To control the gate voltage precisely, a platinum counter-electrode was included to form the standard three-electrode electrochemical configuration[7]. A small a.c. modulation (100 Hz, 0.01 V) was superimposed on the sweeping gate potential (10 mV s^{-1}) and the a.c. current response was measured using a lock-in amplifier (SR850 DSP, Stanford Research Systems). From this the capacitance was determined. In the setup, the dimensions of the connection electrodes were minimized, and the cables and sample holder were carefully shielded to minimize background capacitance. A small residual background capacitance (~1 pF) was determined using a control experiment in which no graphene was present.

Received 22 May 2009; accepted 4 June 2009;
published online 5 July 2009; corrected online 15 July 2009

References

1. Novoselov, K. S. *et al.* Two-dimensional gas of massless Dirac fermions in graphene. *Nature* **438,** 197–200 (2005).
2. Chen, J. H., Jang, C., Xiao, S. D., Ishigami, M. & Fuhrer, M. S. Intrinsic and extrinsic performance limits of graphene devices on SiO_2. *Nature Nanotech.* **3,** 206–209 (2008).
3. Geim, A. K. & Novoselov, K. S. The rise of graphene. *Nature Mater.* **6,** 183–191 (2007).
4. Meric, I. *et al.* Current saturation in zero-bandgap, top-gated graphene field-effect transistors. *Nature Nanotech.* **3,** 654–659 (2008).
5. Schedin, F. *et al.* Detection of individual gas molecules adsorbed on graphene. *Nature Mater.* **6,** 652–655 (2007).
6. Martin, J. *et al.* Observation of electron–hole puddles in graphene using a scanning single-electron transistor. *Nature Phys.* **4,** 144–148 (2008).
7. Das, A. *et al.* Monitoring dopants by Raman scattering in an electrochemically top-gated graphene transistor. *Nature Nanotech.* **3,** 210–215 (2008).
8. Tan, Y. W. *et al.* Measurement of scattering rate and minimum conductivity in graphene. *Phys. Rev. Lett.* **99,** 246803 (2007).
9. Trushin, M. & Schliemann, J. Minimum electrical and thermal conductivity of graphene: a quasiclassical approach. *Phys. Rev. Lett.* **99,** 216602 (2007).
10. Chen, Z. & Appenzeller, J. Mobility extraction and quantum capacitance impact in high performance graphene field-effect transistor devices. *IEEE IEDM Tech. Digest* **21.1,** 509–512 (2008).
11. John, D. L., Castro, L. C. & Pulfrey, D. L. Quantum capacitance in nanoscale device modeling. *J. Appl. Phys.* **96,** 5180–5184 (2004).
12. Fang, T., Konar, A., Xing, H. L. & Jena, D. Carrier statistics and quantum capacitance of graphene sheets and ribbons. *Appl. Phys. Lett.* **91,** 092109 (2007).

13. Giannazzo, F., Sonde, S., Raineri, V. & Rimini, E. Screening length and quantum capacitance in graphene by scanning probe microscopy. *Nano Lett.* **9,** 23–29 (2009).
14. Ishigami, M., Chen, J. H., Cullen, W. G., Fuhrer, M. S. & Williams, E. D. Atomic structure of graphene on SiO_2. *Nano Lett.* **7,** 1643–1648 (2007).
15. Stolyarova, E. *et al.* High-resolution scanning tunneling microscopy imaging of mesoscopic graphene sheets on an insulating surface. *Proc. Natl Acad. Sci. USA* **104,** 9209–9212 (2007).
16. Baldelli, S. Surface structure at the ionic liquid-electrified metal interface. *Acc. Chem. Res.* **41,** 421–431 (2008).
17. Chen, J. H. *et al.* Charged-impurity scattering in graphene. *Nature Phys.* **4,** 377–381 (2008).
18. Adam, S., Hwang, E. H., Galitski, V. M. & Das Sarma, S. A self-consistent theory for graphene transport. *Proc. Natl Acad. Sci. USA* **104,** 18392–18397 (2007).
19. Victor, M. G., Shaffique, A. & Sarma, S. D. Statistics of random voltage fluctuations and the low-density residual conductivity of graphene. *Phys. Rev. B* **76,** 245405 (2007).
20. Ando, T. Screening effect and impurity scattering in monolayer graphene. *J. Phys. Soc. Jpn* **75,** 074716 (2006).
21. Jang, C. *et al.* Tuning the effective fine structure constant in graphene: opposing effects of dielectric screening on short- and long-range potential scattering. *Phys. Rev. Lett.* **101,** 146805 (2008).
22. Cho, S. & Fuhrer, M. S. Charge transport and inhomogeneity near the minimum conductivity point in graphene. *Phys. Rev. B* **77,** 081402 (2008).
23. Randin, J. P. & Yeager, E. Differential capacitance study of stress/annealed pyrolytic graphite electrodes. *J. Electrochem. Soc.* **118,** 711–714 (1971).
24. Bockris, J. O. M. *Modern Electrochemistry: An Introduction to an Interdisciplinary Area* 1st edn (Plenum Press, 1970).
25. Randin, J. P. & Yeager, E. Differential capacitance study on basal plane of stress-annealed pyrolytic-graphite. *J. Electroanal. Chem.* **36,** 257–276 (1972).
26. Chen, F., Xia, J. L. & Tao, N. J. Ionic screening of charged-impurity scattering in graphene. *Nano Lett.* **9,** 1621–1625 (2009).
27. Zhou, S. Y. *et al.* First direct observation of Dirac fermions in graphite. *Nature Phys.* **2,** 595–599 (2006).
28. http://www.semicorp.com.
29. Blake, P. *et al.* Making graphene visible. *Appl. Phys. Lett.* **91,** 063124 (2007).
30. Gao, L. B., Ren, W. C., Li, F. & Cheng, H. M. Total color difference for rapid and accurate identification of graphene. *ACS Nano* **2,** 1625–1633 (2008).

Acknowledgements

We thank the Department of Energy (DE-FG03-01ER45943; J.L.X.) and the National Science Foundation (CHE-0554786; F.C.) for financial support.

Author contributions

J.L.X. carried out the experiments and data analysis. F.C. assisted with the experiments. J.H.L. provided critical sample preparation. N.J.T. conceived the experiment and wrote the manuscript.

Additional information

Supplementary information accompanies this paper at www.nature.com/naturenanotechnology. Reprints and permission information is available online at http://npg.nature.com/reprintsandpermissions/. Correspondence and requests for materials should be addressed to J.L. and N.T.